GEODESIC CURVATURE FLOW ON SURFACES FOR AUTOMATIC SULCAL DELINEATION

Anand A. Joshi[1,3], *David W. Shattuck*[2], *Hanna Damasio*[3] *and Richard M. Leahy*[1]

[1]Signal and Image Processing Institute, University of Southern California, Los Angeles, CA 90089, USA

[2]Laboratory of Neuro Imaging, University of California, Los Angeles, CA 90095, USA

[3]Brain and Creativity Institute, University of Southern California, Los Angeles, CA 90089, USA

ABSTRACT

Sulcal folds (sulci) on the cortical surface are important landmarks of interest for investigating brain development and disease. Accurate and automatic delineation of the sulci is a challenging problem due to substantial variability in their shapes across populations. We present a geodesic curvature flow method for an automatic and accurate delineation of sulcal curves. We assume as input an atlas brain surface mesh on which a set of sulcal curves have been delineated. The sulcal curves are transferred to approximate corresponding locations on the subject brain using a transformation defined by an automatic surface based registration method. The locations of these curves are then refined to follow the true sulcal fundi more closely using geodesic curvature flow on the cortical surface. We present a level set based formulation of this flow on non-flat surfaces which represents the sulcal curves as zero level sets. We also incorporate a curvature based weighting that drives the sulcal curves to the bottoms of the sulcal valleys in the cortical folds. The resulting PDE is discretized on a triangulated mesh using finite elements. Finally, we present a validation by comparing sets of automatically delineated sulcal curves with sets of manually delineated sulcal curves and show that the proposed method is able to find them accurately.

Index Terms— brain imaging, cortical surface, geodesic curvature flow, sulcal curves, level set

1. INTRODUCTION

Human cerebral cortex is often modeled as a highly convoluted sheet of gray matter enclosing the white matter fiber connections. Sulcal folds or sulci are fissures in the cortical surface and are commonly used as surrogates for the cytoarchitectural boundaries in the brain. Therefore sulcal curves are frequently used as landmarks for surface registrations. There is also great interest in analyzing the geometry of these curves directly for studies of disease propagation, symmetry, development and group differences (e.g. [1, 2]). The sulcal curves required for these studies can be produced using manual or automatic delineation, with manual delineation often achieved using interactive software tools [3]. However this can be a tedious and subjective task that also requires substantial knowledge of neuroanatomy. Additionally, intra- and inter-rater variability is introduced in these curves due to subjective choices made by the user. This variability is reduced to some extent using rigorous definitions of a sulcal tracing protocol and extensive training as described in [4, 3]. We previously developed a semiautomatic method using Dijkstra's algorithm to find weighted shortest paths on the cortical surface where the weights depend on curvature [3]. Alternative automatic approaches to sulcal delineation include active shape-based models [5] where sulci are modeled by deforming a surface as opposed to the curves. Another approach involved active shape models [6] where flow of the curves was induced on a spherical parametric representation.

An alternative approach to this problem is to use automatic surface registration to align curvature or depth [7]. Sulcal curves can be delineated on a reference atlas brain surface, which is then aligned with the subject brain surface using automated registration. The sulci from the atlas are then transferred to the subject using the point correspondence defined by the surface mapping. While this approach can find the sulcal location approximately, there is often a significant residual error [4]. This is because automatic methods align the whole surface using curvature and do not focus specifically on the sulcal locations. Also, the variability of the atlas and subject folds can result in the misalignment of sulcal curves, thus the transferred sulcal curves may not lie at the valleys of the subject surfaces. A refinement of these curves can alleviate this problem. This paper describes a new method based on geodesic curvature flow on surfaces where the sulcal curves are represented as curvature weighted geodesics. Geodesic curvature flow was described for parametric surfaces in [8]. Here we present a level set based formulation similar to [9, 10] and apply it to the sulcal detection problem. The sulcal curve evolution is defined in terms of evolution of a zero level set. The flow is discretized in the surface geometry using a finite element method.

2. MATERIALS AND METHODS

We assume, as input, an atlas brain surface mesh with manually delineated sulcal landmarks and a subject brain surface mesh. The goal is to delineate the corresponding sulci on the

This work is supported in part by NIH grants P41 RR013642 and R01 NS074980

subject surface. First, we briefly describe an automated curvature based registration approach that performs alignment of the atlas surface and the subject surface. The sulci from the atlas surface are then transferred to the subject surface, which we refer to as 'RT sulci' (Registration Transfered sulci) henceforth. Then, the RT sulci are adjusted to their correct locations using geodesic curvature flow. We refer to these transferred sulci as 'GCF sulci'.

2.1. Cortical surface registration

We briefly describe our automatic surface registration method, to be published elsewhere, as the main focus of this paper is geodesic curvature flow for sulcal detection. Other automated registration methods could also be used (e.g. FreeSurfer, BrainVISA or BrainVoyager) to transfer the atlas sulcal curves to their initial locations on the subject. We describe a method that establishes one-to-one correspondence between the atlas surface $\mathcal{A}$ and the subject surface $\mathcal{S}$. The method for surface registration has two stages: (i) for each subject, parameterize the surface of each cortical hemisphere to a unit square (ii) find a vector field with respect to this parameterization that aligns curvature of the surfaces. In order to generate such a parameterization, we model the cortical surface as an elastic sheet and solve the associated linear elastic equilibrium equation using the Finite Element Method (FEM) as described in [11]. We constrain the corpus callosum to lie on the boundary of the unit square mapped as a uniform speed curve. Then, an elastic energy minimization yields flat maps of the two cortical hemisphere surfaces to a plane (Fig. 1). A multiresolution representation of curvature for the subject and atlas is calculated. This is then aligned by minimizing a cost function with elastic energy as a regularizing penalty. The registration is made more robust by adding 3D coordinate matching as a mismatch penalty along with the curvature. This performs reparameterization of the cortical hemisphere surfaces and establishes a one to one point correspondence between subject and atlas surfaces. We used the BrainSuite software [12] to extract the tessellated cortical surface meshes for the atlas and for each subject from T1-weighted MRI volumes, as well as to interactively trace 26 candidate sulcal curves on the atlas brain according to the protocol described in [4]. By using the point correspondence established using the registration, these curves are then transferred to the subject surfaces. The objective of the geodesic curvature flow method presented in the next section is to perform refinement of these RT sulci to find accurate sulcal curves in the subjects surface.

2.2. Finite element method

We use an FEM-based level set approach for computing the curvature flow, as we describe in Sec 2.3. We first describe how we perform FEM discretization on a triangulated mesh of the partial derivatives [13]. Let α be any piecewise linear real-valued scalar function defined over the surface, and let x, y

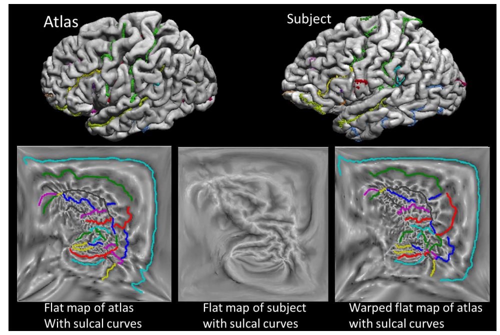

Fig. 1. Curvature based automatic surface registration

denote local coordinates for triangle i. We can also denote the local coordinates of the three vertices of the triangle as (x_1, y_1), (x_2, y_2) and (x_3, y_3) respectively. Since α is linear on the i^{th} triangle, we can write,

$$\alpha(x, y) \quad = \quad a_0^i + a_1^i x + a_2^i y. \tag{1}$$

Writing this expression at three vertices of the triangle i in matrix form yields

$$\underbrace{\begin{pmatrix} 1 & x_1^i & y_1^i \\ 1 & x_2^i & y_2^i \\ 1 & x_3^i & y_3^i \end{pmatrix}}_{D^i} \begin{pmatrix} a_0^i \\ a_1^i \\ a_2^i \end{pmatrix} = \begin{pmatrix} \alpha^i(x_1, y_1) \\ \alpha^i(x_2, y_2) \\ \alpha^i(x_3, y_3) \end{pmatrix}. \tag{2}$$

The coefficients a_0^i, a_1^i and a_2^i can be obtained by inverting the matrix D^i. From Eq. 1 and by inverting the matrix in Eq. 2, we obtain

$$\begin{pmatrix} \frac{\partial \alpha^i}{\partial x} \\ \frac{\partial \alpha^i}{\partial y} \end{pmatrix} = \begin{pmatrix} a_1^i \\ a_2^i \end{pmatrix} = \frac{1}{|D^i|} \begin{pmatrix} y_2^i - y_1^i & y_3^i - y_1^i & y_1^i - y_2^i \\ x_1^i - x_2^i & x_1^i - x_3^i & x_2^i - x_1^i \end{pmatrix} \begin{pmatrix} \alpha^i(x_1, y_1) \\ \alpha^i(x_2, y_2) \\ \alpha^i(x_3, y_3) \end{pmatrix}.$$

Denote the discretization of $\frac{\partial}{\partial x}$ and $\frac{\partial}{\partial y}$ at triangle i by D_x^i and D_y^i respectively. Also note that $|D^i| = 2A_i$ where A_i is area of the i^{th} triangle. Then we have:

$$\begin{aligned} D_x^i &= \frac{1}{2A_i} \begin{pmatrix} y_2^i - y_1^i & y_3^i - y_1^i & y_1^i - y_2^i \end{pmatrix}, \\ D_y^i &= \frac{1}{2A_i} \begin{pmatrix} x_1^i - x_2^i & x_1^i - x_3^i & x_2^i - x_1^i \end{pmatrix}. \end{aligned}$$

These triangle-wise derivative operators can be assembled over the entire surface and can be written as D_x and D_y matrices. The derivative operator matrix is thus denoted by $D = [D_x, D_y]^T$.

2.3. Geodesic curvature flow on surfaces

The RT curves are typically in the correct sulcal valley, but are not exactly at their desired locations at the bottoms of these valleys. We have found that sulci propagated by automatic registration generally lie within 3cm of the true sulcal valleys [4]. Therefore, to reduce the computational load, we calculate a surface patch around the sulcus of interest using front propagation for 3cm (Fig. 2).

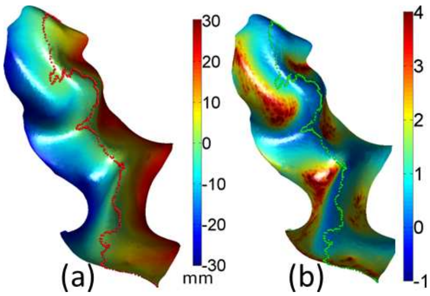

Fig. 2. (a) Initial sulcal curve and signed distance function; (b) curvature weighting function f shown as color-coded overlay on the surface patch around that sulcus.

The geodesic curvature flow is performed over this surface patch around the sulcus of interest using a level set formulation. The approach presented here is based on [10], but in our case we add curvature weighting when computing minimizing geodesics. Assume $\mathcal{M}$ is a general 2D manifold representing the surface patch embedded in $\mathbb{R}^3$ and let Γ be the sulcal curve on the surface. Let the curve Γ be represented by the zero level set of a function $\phi : \mathcal{M} \to \mathbb{R}$, i.e., $\Gamma = \{s : \phi(s) = 0\}$. Suppose that $c : \mathcal{M} \to \mathbb{R}$ is the curvature of the surface $\mathcal{M}$. We have found that, for sulcal tracing, a sigmoid function of the curvature works well as weights on the paths for sulcal tracing [3]. Therefore, we define $f(s) = \frac{1}{1+e^{-2c(s)}}$ as the curvature based weights on the surfaces. We seek to minimize the weighted length of Γ given by $E(\Gamma) = \int_{\Gamma:\phi=0} f dS$, where integration is computed over the surface at the curve points. Following [10, 8, 9], the Euler-Lagrange equations for the energy functional minimization of $E(\Gamma)$ yield

$$\begin{cases} -\text{div}\left(f\frac{\nabla\phi}{|\nabla\phi|}\right) & = 0 \\ \frac{\partial\phi}{\partial\vec{n}}|_{\partial\mathcal{M}} & = 0, \end{cases}$$

where $\partial\mathcal{M}$ is the boundary of $\mathcal{M}$ and $\vec{n}$ is the intrinsic outward normal of $\partial\mathcal{M}$. A gradient descent flow of the equation [14] is given by:

$$\begin{cases} \frac{\partial\phi}{\partial t} = |\nabla\phi|\text{div}\left(f\frac{\nabla\phi}{|\nabla\phi|}\right) \\ \frac{\partial\phi}{\partial\vec{n}}|_{\partial\mathcal{M}} = 0 \\ \phi(0) = \phi_0 \end{cases}$$

where we choose ϕ_0 to be a signed distance function from the initial sulcal curve. The boundary condition is discretized in a standard way in the finite element formulation and we refer the reader to [13] for details. Next, we use the divergence identity,

$$\text{div}\,(f\nabla\phi) = \text{div}\left(f\nabla\phi\frac{|\nabla\phi|}{|\nabla\phi|}\right) = f\frac{\nabla\phi\cdot\nabla(|\nabla\phi|)}{|\nabla\phi|} + |\nabla\phi|\text{div}\left(f\frac{\nabla\phi}{|\nabla\phi|}\right).$$

This gives

$$\begin{cases} \frac{\partial\phi}{\partial t} = \text{div}\,(f\nabla\phi) + g(\phi) \\ g(\phi) = -f\frac{\nabla\phi}{|\nabla\phi|}\cdot\nabla\left(|\nabla\phi|\right) \\ \phi(0) = \phi_0 \end{cases}$$

By using discretization of derivatives in Sec. 2.2 and after performing implicit-explicit discretization of the time derivative, we get:

$$\frac{\phi^n - \phi^{n-1}}{\Delta t} + \frac{D\cdot(fD\phi^n) + D\cdot(fD\phi^{n-1})}{2} = Ag(\phi^{n-1}).$$

Let $B = D\cdot fD$ be the weighted mass matrix and A be the load matrix, such that for triangle i, $A^i = \frac{Area_i}{12}\begin{pmatrix}2&1&1\\1&2&1\\1&1&2\end{pmatrix}$.

Therefore, in matrix form, we get

$$B\phi^n + \frac{1}{2}\Delta tA\phi^n = B\phi^{n-1} - \frac{1}{2}\Delta tA\phi^{n-1} + \Delta tBg(\phi^{n-1}).$$

Finally, after simplification, the curve evolution problem reduces to solving a linear matrix equation given by:

$$\phi^n = (B + \frac{1}{2}\Delta tA)^{-1}\left((B - \frac{1}{2}\Delta tA)\phi^{n-1} + \Delta tBg(\phi^{n-1})\right).$$

This system of equations is solved using a preconditioned conjugate gradient method with Jacobi preconditioner. The algorithm was implemented in Matlab. We choose $\Delta t = .5$ and the number of iterations $N_{iter} = 20$. The algorithm takes approximately 1 hour per subject hemisphere for the refinement of all the sulci on an 8 core Intel i7 computer. The final GCF curves were extracted by finding the zero level set of the function ϕ after 20 iterations.

3. RESULTS

In order to evaluate the performance of the method, we performed validation on a set of 12 subject brains. We used the ICBM Single Subject Template as our atlas (http://www.loni.ucla.edu/Atlas We applied the BrainSuite software [12] to extract cortical surface meshes from the subject and atlas MRI data. BrainSuite includes a multistage cortical modeling sequence. First the brain is extracted from the surrounding skull and scalp tissues using a combination of edge detection and mathematical morphology. Next the intensities of the MRI are corrected for shading artifacts. Each voxel in the corrected image is then labeled according to tissue type using a statistical classifier. A standard atlas with associated structure labels is aligned to the subject volume, providing a label for cerebellum, cerebrum, brainstem, and subcortical regions. These labels are combined with the tissue classification to automatically identify the cerebral white matter, to fill the ventricular spaces, and to remove the brainstem and cerebellum. This produces a volume whose boundary surface represents the outer white-matter surface of the cerebral cortex. Prior to tessellation, the topological defects are identified and removed automatically from the binary volume using a graph based approach. A tessellated isosurface of the resulting mask is then extracted to produce a genus zero surface. This surface is then expanded to identify the pial surface, i.e., the boundary between grey matter and CSF. The surfaces are then split into left and right hemispheres based on the registered atlas labels.

We delineated sulcal curves using BrainSuite's interactive delineation tools [3] following a sulcal protocol with 26

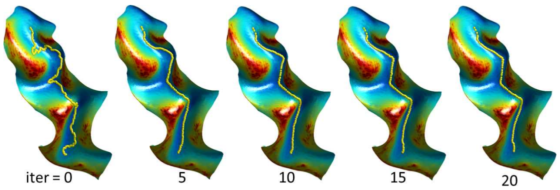

Fig. 3. Evolution of the sulcal curve by geodesic curvature flow for different iterations. The curvature weighting function f is shown as color-coded overlay

	manual vs RT(mm)	manual vs GCF(mm)
Cent. sulcus	1.8(L), 2.1(R)	1.4(L), 1.4(R)
Sup. Front. sulcus	2.7(L), 2.7(R)	1.8(L), 1.3(R)
Calc. sulcus	2.3(L), 2.3(R)	2.0(L), 2.1(R)
Sup. Temp. sulcus	4.2(L), 4.1(R)	3.5(L), 3.6(R)
Avg over all 26 sulci	3.6(L), 3.9(R)	2.7(L), 3.3(R)

Table 1. Sulcal errors between manually delineated curves and automatically generated curves by registration and transfer (RT) and geodesic curvature flow refinement (GCF) measured by Hausdorff distance metric. The table shows mean error for cortical delineation of 12 subjects for both left (L) and right (R) hemispheres.

sulcal curves [4]. These sulci are consistently seen in normal brains, and are distributed throughout the entire cortical surface. A thorough description of the sulcal curves with instructions on how to trace them is available on our web site (http://neuroimage.usc.edu/CurveProtocol.html). We traced the curves on the midcortical surface because it provides better access to the depth of the sulci than the pial surface, and the valleys of the sulci are more convex than the white matter surface allowing more stable tracing of the curves. The same procedure was repeated on the single subject atlas. Next, we performed the subject to atlas registration as described in Sec. 2.1 and transferred the curves of the atlas to the subject brains. The transferred curves were refined using the geodesic curvature flow as discussed in Sec 2.3. The evolution of one sulcal curve in shown in Fig. 3 (see http://sipi.usc.edu/~ajoshi/GCF_Sulci.html for an animation).

To compare the alignment of transferred curves, as well as GCF curves, we mapped the 26 protocol curves from all subjects to the target surface. We then quantified their accuracy using their variance on the subject surface, which is estimated as follows. We use a distance measure based on the Hausdorff distance metric:

$$d(D_i, D_j) = 0.5\frac{1}{N}\sum_{p\in D_i}\min_{p\in D_i}|p-q| + 0.5\frac{1}{N}\sum_{p\in D_j}\min_{q\in D_j}|p-q|$$

where $d(D_i, D_j)$ is the distance between the pointsets on triangle mesh representing curves D_i and D_j. This distance is computed between subject's manual curve and RT curve, as well as manual curve and GCF curve.

The results for some of the prominent sulci are presented in Table 1. It can be seen that the sulcal error is reduced substantially after geodesic curvature flow. This improvement is most pronounced in the sulci that are clearly defined by curvature extrema and shortest length paths on the cortex, such as central sulcus and superior frontal sulcus.

4. CONCLUSION

This paper presents a method for accurate and automatic delineation of sulcal curves on human brain cortex which are important inputs for cortical shape analysis. We will test this method further with brains with disorders, but preliminary results show promising prospects for the method in case of small temporal lobe lesions. The level set approach and FEM formulation allowed us to perform geodesic curvature flow on the surface. We demonstrated the potential benefit of this method by applying it to a small population of brains and showed that the GCF curves are significantly more accurate than the RT curves. A more extensive validation is planned.

5. REFERENCES

[1] M.E. Rettmann, M.A. Kraut, J.L. Prince, and S.M. Resnick, "Cross-sectional and longitudinal analyses of anatomical sulcal changes associated with aging," *Cerebral Cortex*, vol. 16, no. 11, pp. 1584–1594, 2006.

[2] K. Narr, P. Thompson, T. Sharma, J. Moussai, C. Zoumalan, J. Rayman, and A. Toga, "Three-dimensional mapping of gyral shape and cortical surface asymmetries in schizophrenia: gender effects," *Am. J. Psychiatry*, vol. 158, no. 2, pp. 244–255, Feb 2001.

[3] D.W. Shattuck, A.A. Joshi, D. Pantazis, E. Kan, R.A. Dutton, E.R. Sowell, P.M. Thompson, A.W. Toga, and R.M. Leahy, "Semi-automated method for delineation of landmarks on models of the cerebral cortex," *J neuroscience meth*, vol. 178, no. 2, pp. 385–392, 2009.

[4] D. Pantazis, A. Joshi, J. Jiang, D.W. Shattuck, L.E. Bernstein, H. Damasio, and R.M. Leahy, "Comparison of landmark-based and automatic methods for cortical surface registration," *Neuroimage*, vol. 49, no. 3, pp. 2479–2493, 2010.

[5] M. Vaillant and C. Davatzikos, "Finding parametric representations of the cortical sulci using an active contour model," *Medical Image Analysis*, vol. 1, no. 4, pp. 295–315, 1997.

[6] X. Tao, J.L. Prince, and C. Davatzikos, "Using a statistical shape model to extract sulcal curves on the outer cortex of the human brain," *Medical Imaging, IEEE Transactions on*, vol. 21, no. 5, pp. 513–524, 2002.

[7] B. Fischl, M. I. Sereno, R. B. H. Tootell, and A. M. Dale, "High-resolution intersubject averaging and a coordinate system for the cortical surface," *Human Brain Mapping*, vol. 8, pp. 272–284, 1998.

[8] A. Spira and R. Kimmel, "Geodesic curvature flow on parametric surfaces," *Curve and Surface Design*, pp. 365–373, 2002.

[9] C. Wu and X. Tai, "A level set formulation of geodesic curvature flow on simplicial surfaces," *Visualization and Computer Graphics, IEEE Transactions on*, vol. 16, no. 4, pp. 647–662, 2010.

[10] R. Lai, Y. Shi, N. Sicotte, and A.W. Toga, "Automated corpus callosum extraction via laplace-beltrami nodal parcellation and intrinsic geodesic curvature flows on surfaces," in *ICCV*, 2011.

[11] A. A. Joshi, D. W. Shattuck, P. M. Thompson, and R. M. Leahy, "Surface-constrained volumetric brain registration using harmonic mappings," *IEEE Trans. Med. Imag*, vol. 26, no. 12, pp. 1657–1669, 2007.

[12] D. W. Shattuck and R. M. Leahy, "BrainSuite: An automated cortical surface identification tool," *Medical Image Analysis*, vol. 8, no. 2, pp. 129–142, 2002.

[13] M.N.O. Sadiku, *Numerical techniques in electromagnetics*, CRC, 2000.

[14] L.T. Cheng, P. Burchard, B. Merriman, and S. Osher, "Motion of curves constrained on surfaces using a level-set approach," *Journal of Computational Physics*, vol. 175, no. 2, pp. 604–644, 2002.